Electronic Supplementary Material (ESI) for Lab on a Chip.
This journal is © The Royal Society of Chemistry 2019

Supporting Information for:

An integrated device for the rapid and sensitive detection of the influenza hemagglutinin

Caitlin E. Anderson[1], Joshua R. Buser[1], Alexis M. Fleming[1], Eva Maria Strauch[2], Paula D. Ladd[2], Janet Englund[3], David Baker[2], and Paul Yager[1]

[1]*Department of Bioengineering, University of Washington, Seattle, WA*

[2]*Department of Biochemistry, University of Washington, Seattle, WA*

[3]*Seattle Children's Research Institute, Seattle, WA*

Table of contents

Figure S1. Drawing of 2DPN device with dimension……………………………………..……S-2
Table S1. Optimization of pinch valve for amplification buffer release……………....S-2
Figure S2. Schematic of comb devices used for rapid assay development………… S-3
Figure S3. Viral lysis eliminates signal from influenza virus assay………………….. S-3
Figure S4. Specificity testing for strains of influenza A and B ………………………... S-4
Figure S5. Limit of detection analysis for H1N1 and H3N2 viruses …………………... S-5
Figure S6. Limit of detection analysis by viral RNA content …………………………... S-6
Figure S7. Trehalose optimization in conjugate pad ………………………………………… S-7
Figure S8. Conjugate optimization in conjugate pad ………………………………………… S-8
Figure S9. Limit of detection analysis by infectious unit amount ……………………… S-8

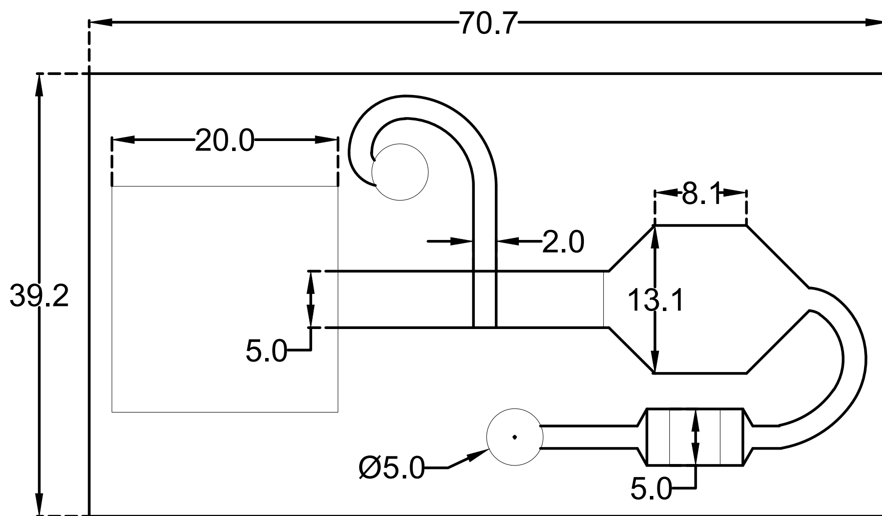

Figure S1. Drawing of 2DPN device with dimensions shown in mm. The 2DPN components consist of glass fiber, nitrocellulose, and cellulose as shown in Figure 1 of the main text.

Table S1. Optimization of pinch valve for amplification buffer release. By varying the width of water soluble (WS) paper release, the timing of delivery of amplification buffer varies between 21 and 40 minutes.

Spy WS paper width	8 mm	9mm	10mm
Rep 1	23	29	48
Rep 2	23	28	47
Rep 3	17	24	39
Rep 4	24	31	33
Rep 5	18	35	37
Average	21	29.4	40.8
Std Dev	2.898275349	3.611094017	5.810335619
Percent deviation	13.8%	12.3%	14.2%

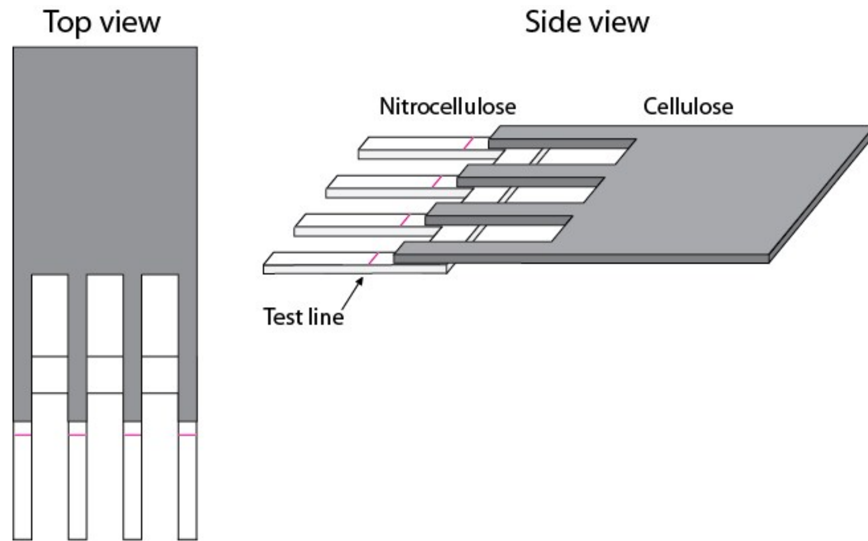

Figure S2. Schematic of the comb devices used for rapid assay development in the dipstick format. Comb devices consist of nitrocellulose that has been spotted with a test line, and cellulose that is aligned and held in contact with the nitrocellulose using a custom made plastic holding card.

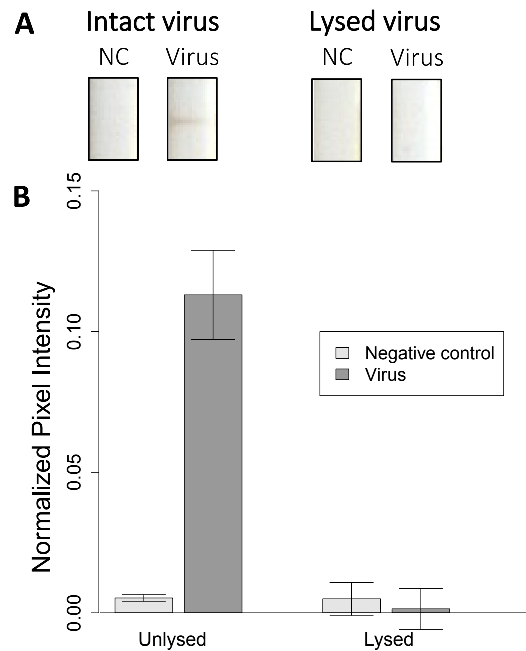

Figure S3. Loss of signal in the presence of 5% Triton X-100 (a viral lysis agent), suggesting that assay performance is dependent upon the intact form of the influenza virus. This concentration has previously been demonstrated to lyse the influenza virus [7]. (A) Representative scans of all four conditions, each of which was run with an n=4. (B) Normalized pixel intensity of the scanned images for both lysed and unlysed influenza virus.

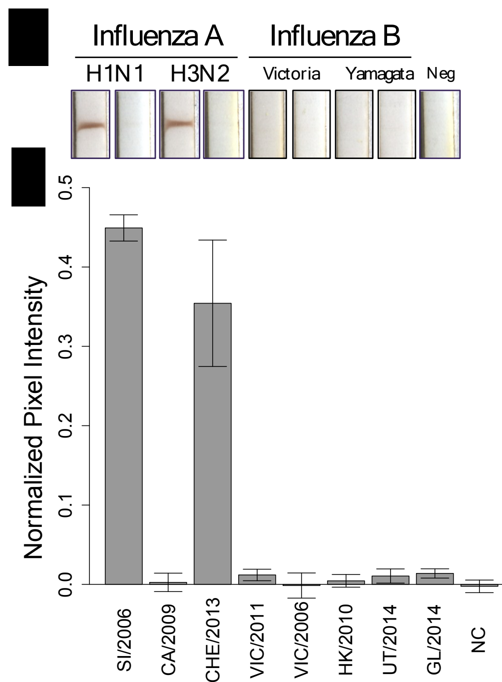

Figure S4. Specificity testing of the hemagglutinin assay for a panel of influenza A and B strains of the virus. Detection of two specific strains of influenza A is shown, specifically the Solomon Islands strain of H1N1 and the Switzerland 2013 strain of H3N2. No cross reactivity was seen with the influenza B strains. Representative test lines and the normalized pixel intensity are included. Each strain was tested with n=4 replicates.

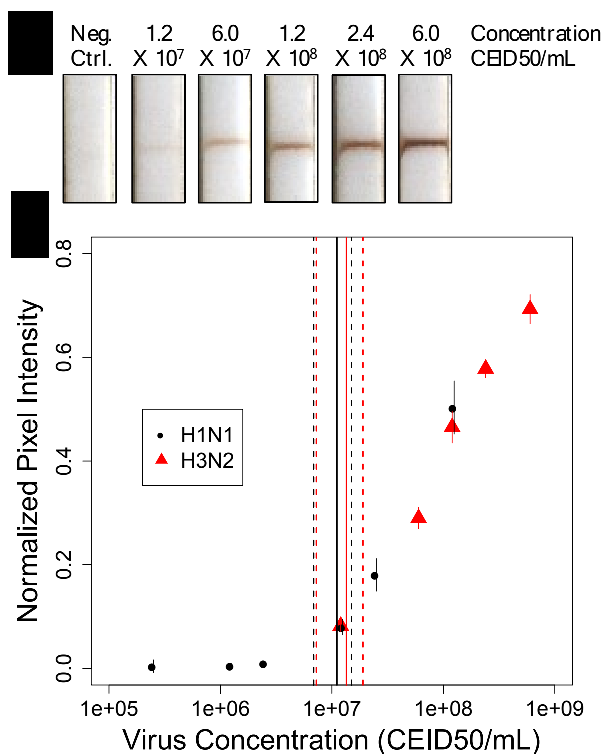

Figure S5. Limit of detection analysis for H1N1 and H3N2 strains. (A) Scans of example test strips run in the dipstick format. (B) Normalized pixel intensity for both strains of virus. Each condition was tested with n=4 replicates. The limits of detection were found to be 1.35 x 10^7 $CEID_{50}$/mL (95% CI: [7.26 x 10^6,1.90 x 10^7]) and 1.11 x 10^7 $CEID_{50}$/mL (95% CI: [6.85 x 10^6, 1.50 x 10^7]) respectively. The solid lines indicate the calculated LOD, while the dashed lines indicate the 95% confidence interval.

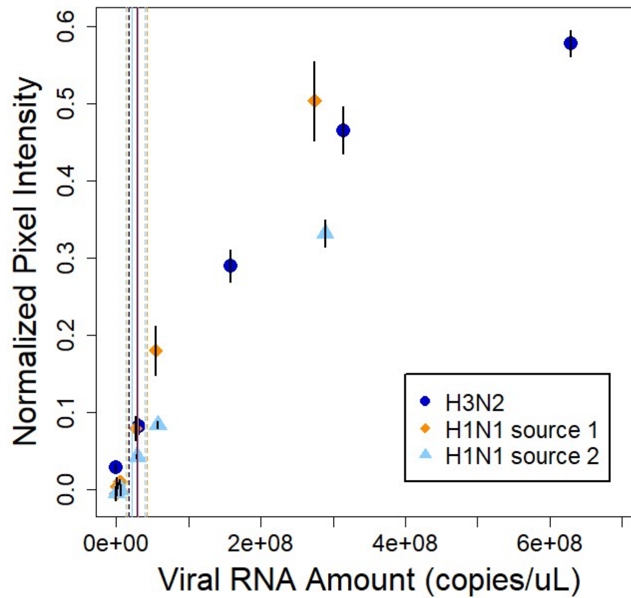

Figure S6. Limit of detection for the flu assay by viral RNA amount for the three virus stocks tested. Viral RNA amount was determined using qRT-PCR for each source of virus. The limits of detection for these three virus strains were found to be statistically similar, as depicted by the LOD (line) and 95% CI (dotted line). The LODs are 2.91×10^7 copies/µL [1.80×10^7, 3.94×10^7], 2.96×10^7 copies/uL [1.59×10^7, 4.17×10^7], and 2.10×10^7 copies/µL [1.38×10^7, 3.98×10^7] for the H3N2, H1N1 source 1, and H1N1 source 2 respectively. The H3N2 and H1N1 source 1 virus stocks were obtained from the Influenza Reagent Resource. H1N1 source 2 was grown in the Bloom lab at the University of Washington.

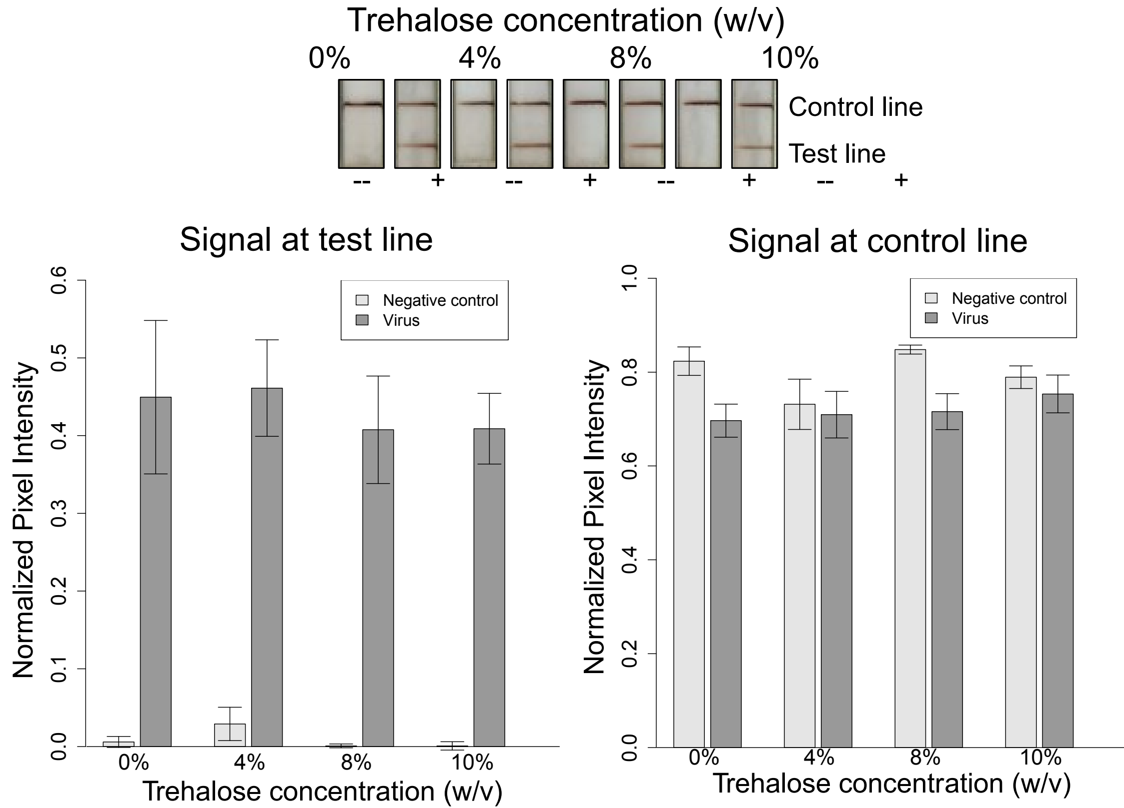

Figure S7. Optimization of the concentration of trehalose included in the dry storage mixture prior to lyophilization. Scanned images (at 600 dpi) and normalized pixel intensity of the test and control line on these devices were run to test the effect of trehalose concentration in the dry storage mix. Dry storage pads were prepared, lyophilized, and stored in the desiccator at room temperature (25°C) overnight before testing. Four concentrations of trehalose were tested, 0, 4, 8, and 10% with both virus and PBST with an n=3 for each concentration.

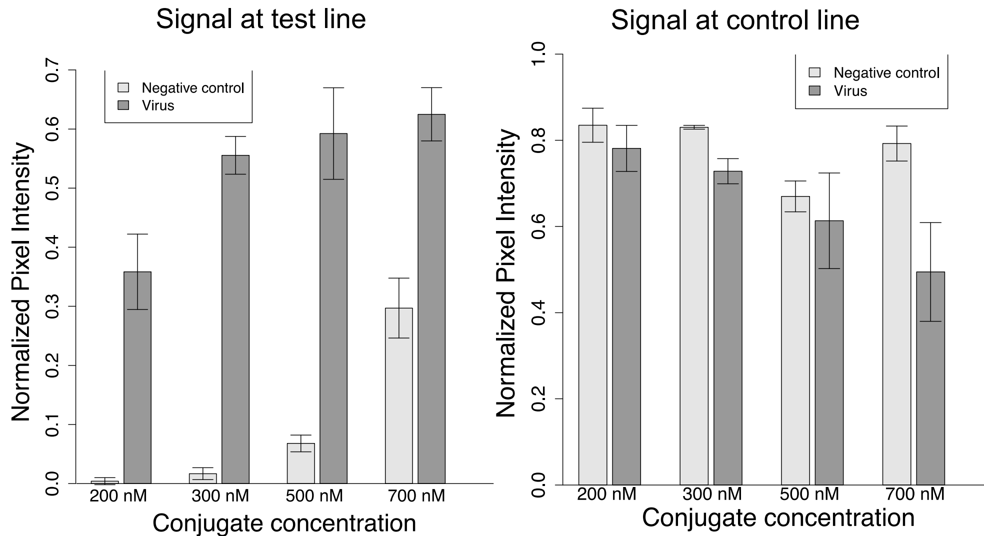

Figure S8. Concentration optimization of hemagglutinin binder-HRP conjugate. Optimizing primarily with the test line in mind (left), we found the optimal concentration of conjugate to be around 300 nM based on the difference in signal between the negative and the positive. At the control line (right), we found that higher concentrations of conjugate led to lower signal in the presence of virus. The normalized pixel intensity was calculated for both the test line and control line. All conditions were tested with an n=4.

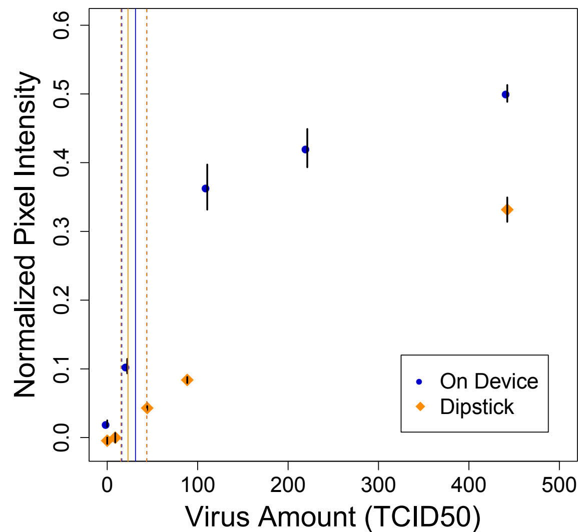

Figure S9. Determination of the limit of detection for the device (blue) and dipstick (orange) assays for virus amount ($TCID_{50}$) instead of concentration, as found in the main text. (A) Representative scans of device test strips. (B) Normalized pixel intensity for the assay run on device and in the dipstick format. The limits of detection were found to be 31.22 $TCID_{50}$ (95% CI: [16.03, 43.82]) and 23 $TCID_{50}$/mL (95% CI: [15.12, 43.6]) in the on device and dipstick formats respectively. The solid lines indicate the calculated LOD, while the dashed lines indicate the 95% confidence interval. Data points are mean ± standard error, n=6.